A 60 GHz Wireless Home Area Network With Radio Over Fiber Repeaters

Joffray Guillory, Eric Tanguy, Anna Pizzinat, *Member, IEEE*, Benoît Charbonnier, Sylvain Meyer, Catherine Algani, and Hongwu Li

***Abstract*—Home area networks will have to deal with the future multigigabit wireless systems that are emerging or are under development. These millimeter-wave radio systems achieve data rates up to several Gb/s per channel, but over short distance. So, to expand the radio coverage, we propose to introduce a radio-over-fiber (RoF) infrastructure at home. This paper presents a complete study of a RoF system: the 60 GHz radio coverage is extended using a RoF link working at intermediate frequency with two hops in the air. An experimental setup of such an infrastructure has been realized and characterized. A low-cost solution, working at 850 nm, was chosen using multimode fiber and off-the-shelf millimeter-wave and photonic components. Finally, a real-time transmission between two commercial WirelessHD devices working at 3 Gb/s has been carried out.**

***Index Terms*—Home area network (HAN), IEEE 802.15.3c, IEEE 802.11ad, optical architecture, optical transducers, radio over fiber (RoF), WirelessHD.**

I. Introduction

THE EVOLUTION of the home area network (HAN) is determined by several trends [1]. A major one is the proliferation of connected devices in the home, used increasingly and simultaneously via wireless ultrahigh data rate connection. The current generation of WiFi systems (IEEE 802.11n) can achieve theoretically 600 Mb/s [2], but new radio standards allowing higher data rates have emerged or are under development. All these new standards address the unlicensed millimeter-wave band from 57 to 66 GHz as shown in Fig. 1. In this band, divided into four 2.16 GHz-bandwidth channels, it is possible to achieve bit rates up to 7 Gb/s per channel (see Table I). IEEE 802.15.3c [3] and WirelessHD [4] standards were finalized in 2009 and are devoted to wireless personal area network communication. More recently, the IEEE 802.11ad [5] group has been created by WiGig consortium [6]: it addresses networking with wireless local area network systems and targets WiFi Alliance certification. As a consequence, IEEE 802.11ad should lead the multigigabit wireless systems race. 60 GHz technologies are now mature: WirelessHD devices are already available in the market for wireless high-definition multimedia interface (HDMI) applications and IEEE 802.11ad products could be available by the end of 2011.

Channel Number	Low Freq. (GHz)	Center Freq. (GHz)	High Freq. (GHz)
A1	57.240	58.320	59.400
A2	59.400	60.480	61.560
A3	61.560	62.640	63.720
A4	63.720	64.800	65.880

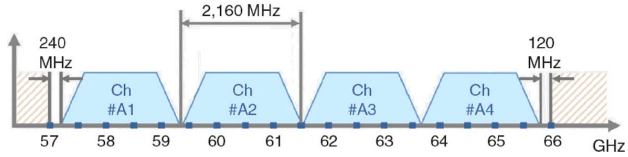

Fig. 1. Channelization of the 60 GHz band in Europe [7], [8].

However, the limitation of these systems is their short range due to the high-propagation attenuation and to the fact that signals in the 60 GHz band cannot cross the walls. Consequently, their coverage is limited to a single room and to a small indoor open area. The main challenge is to find solutions to ensure the coverage of the entire HAN, and to interconnect all the devices located in different rooms. In this paper, we propose to solve this problem by means of the radio-over-fiber (RoF) technology distributing 60 GHz radio signal to several access points spread around the home. Compared to other techniques, RoF is advantageous because of its capability of supporting multistandard systems due to its transparency to the radio protocol and to the modulation format. Moreover, an HAN based on an optical fiber infrastructure is future proof for the following aspects: higher data rate, delivery of a multiplicity of high-performance parallel services [9], high quality of service and minimization of the exposure to the electromagnetic field. Several studies have already been carried out on RoF for 60 GHz applications, principally on long-term-related topics [10], [11], such as optical frequency upconversion for millimeter-wave signals generation [12] and high-speed Mach–Zehnder Modulators [13], [14]. From the viewpoint of the HAN market, a RoF system can represent a competitive solution only if it is easy to deploy and the necessary transceivers are low cost and compact. In this paper, we address these issues on the basis of a system in which the 60 GHz radio signals are distributed over fiber at intermediate frequency (IFoF). In a previous paper [15], we

J. Guillory, A. Pizzinat, B. Charbonnier, and S. Meyer are with France Télécom R&D—Orange Labs, 22300 Lannion, France (e-mail: joffray.guillory@orangelabs-ftgroup.com; anna.pizzinat@orange-ftgroup.com; benoit.charbonnier@orange-ftgroup.com; sylvain.meyer@orange-ftgroup.com).

E. Tanguy and H. W. Li are with the Institut de Recherche en Electrotechnique et Electronique de Nantes Atlantique, University of Nantes, 44300 Nantes, France (e-mail: Eric.Tanguy@univ-nantes.fr; Hongwu.Li@univ-nantes.fr).

C. Algani is with ESYCOM laboratory, Conservatoire National des Arts et Métiers, 75003 Paris, France (e-mail: catherine.algani@cnam.fr).

TABLE I
RADIO STANDARD PROPERTIES WITH YEAR OF REALIZATION, DATA RATES, AND INDUSTRIAL PRODUCTS OUTLOOK

IEEE 802.15.3c	WirelessHD	IEEE 802.11ad
2009	2009	2012
20 to 5,670 Mbit/s	952 to 7,138 Mbit/s	385 to 6,757 Mbit/s
Future likely to be compromised	Based on IEEE 802.15.3c A/V mode	Should lead the market with Wi-Fi certification

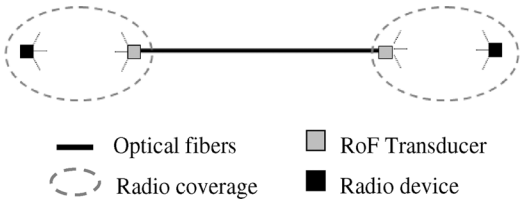

Fig. 2. Point-to-point RoF link: the optical tunnel.

have demonstrated that the direct optical distribution of millimeter-wave radio signals and IFoF distribution lead to comparable performances, but the cost of the system is drastically reduced in the second case. In this paper, we go further by presenting, for the first time to our knowledge, experimental results on the transmission of multigigabit orthogonal frequency division multiplexing (OFDM) signals at 60 GHz, by using a RoF tunnel. In other terms, after propagation over a first wireless link, the 60 GHz signal is downconverted at IF and used to modulate a laser diode for transmission over multimode fiber (MMF); after photodetection, the signal is upconverted to 60 GHz and retransmitted over a second wireless link.

This paper is organized as follows: after a short presentation of the optical tunnel (or repeater) and the IFoF transducers in Section II, we determine, in Section III, the best electrical and optical parameters in order to optimize the RoF link. Afterward, we characterize the proposed RoF infrastructure, building the architecture step by step: to the direct millimeter-wave radio link characterized first as the baseline, we add an electrical repeater, and finally we introduce the RoF repeater. As a final point, we show a real-time transmission between two commercial WirelessHD devices using a wireless link including a RoF tunnel.

II. RoF for the HAN

In previous papers, we have proposed and studied several RoF architectures [16], [17]. A very simple case is the optical tunnel shown in Fig. 2.

This optical link acts as a transparent radio repeater; indeed, the radio signal captured at the input is transmitted to the output of the tunnel. This scheme is advantageous because two wireless devices in two rooms separated by wall(s) can communicate as if they were visible to one another. At the same time, it is quite challenging for the RoF system due to the high and strongly variable losses and the distortions introduced by the two air links. Moreover, the demonstration of the feasibility of the optical tunnel is also the first step toward the implementation of multipoint-to-multipoint networks [17]. As a consequence, in the following, we focus on the optical tunnel architecture.

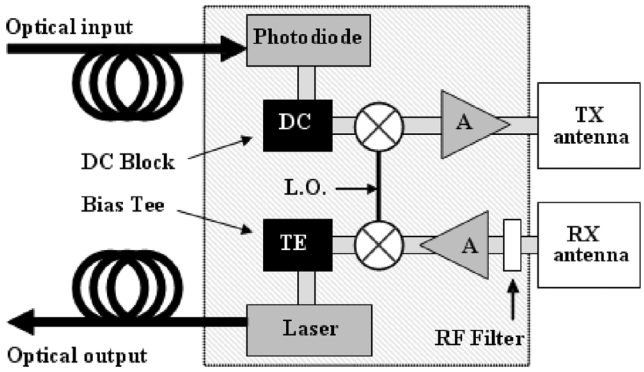

Fig. 3. RoF transducer in intermediate frequency configuration.

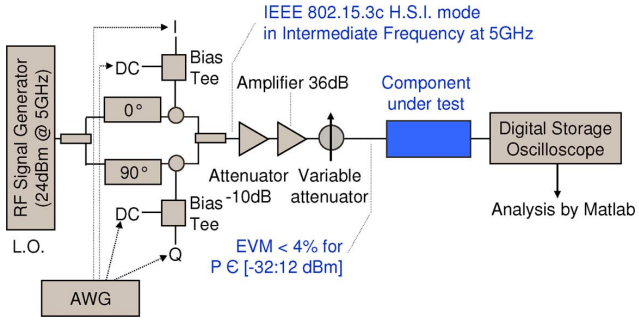

Fig. 4. Experimental test bench of radio OFDM signal generation at IF = 5 GHz.

As anticipated in the previous section, to remain low cost, a RoF system for HAN applications has to be built with very simple and cheap bricks. The RoF transducers, key elements realizing electro-optic (E/O) and opto-electronic (O/E) conversions, are composed of two antennas, a laser diode, a photodiode, and RF amplifiers (see Fig. 3). Low cost vertical-cavity surface-emitting lasers (VCSELs) emitting at 850 nm and GaAs PIN photodiodes with built-in transimpedance amplifier (TIA), developed for 10 Gb/s digital communications over 50 μm MMF by Finisar, are chosen. Because of their bandwidth limited below 10 GHz, RoF transducers also need a local oscillator (LO) and associated mixers to transpose the millimeter-wave signal at IF before the laser direct modulation and to bring back the signal at 60 GHz after the photodetection for radio reemission. Finally, the antennas incorporated in the RoF transducers are horn antennas. Smart antennas performing beamforming within a room should improve the system; further investigations will be carried out on this topic.

III. Characterization of the Link With an IFoF

The experimental setup has been built step by step in order to determine the impact of each element in the link. First, we have characterized the propagation of a radio signal over fiber by means of the experimental setup shown in Fig. 4.

A 3.08 Gb/s pseudorandom OFDM baseband signal modulated with a quadrature phase-shift keying (QPSK) scheme is generated under MATLAB according to the high-speed interfaces (HSI) mode of the IEEE 802.15.3c standard. This baseband signal is fed into a 10 GSa/s arbitrary waveform generator

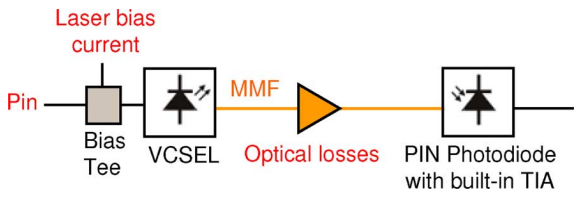

Fig. 5. RoF link to be placed as the "component under test" in Fig. 4.

(AWG). The generated in-phase (I) and quadrature (Q) components are transposed to IF by mixing with an RF oscillator split in two paths with a 90° phase shift. Finally, the two components are combined by an RF coupler to create the IF-OFDM input signal. A real-time digital storage oscilloscope, with 13 GHz bandwidth and 40 GSa/s speed, receives the transmitted signal through the system for analysis under MATLAB and calculation of the link error vector magnitude (EVM).

The direct link or back-to-back connection, i.e., the oscilloscope simply connected to the IF-OFDM signal generator, presents an EVM lower than 4% for an input power range of 44 dB, varying from -32 to $+12$ dBm, thanks to cascaded amplifiers and attenuators that control precisely the RF input power of the system. Note that the oscilloscope accepts a wide range of input power and automatically adjusts the signal level. This configuration and the corresponding EVM value are considered as a reference in order to make proper comparisons with the different tested configurations.

Before going to the complete optical tunnel setup, we characterize separately the RoF and wireless links in order to analyze the influence of each part of the complete architecture. The RoF link shown in Fig. 5 is composed of the optoelectronic components described in Section II and of a 1 m length MMF. A variable optical attenuator is introduced in the RoF link to analyze the effect of additional optical losses due to fiber attenuation, fiber bends, and optical splitters [17].

A. Analog Characterization of the RoF Link

The link has been characterized in terms of relative intensity noise (RIN) and nonlinearity. For RF up to 10 GHz and in the linear part of the VCSEL static characteristic (i.e., 6.5 mA bias current), the measured RIN is lower than -130 dBc/Hz, even at the frequency relaxation oscillation (4.5 GHz). At 3 GHz, with no optical loss and for the same laser bias current, an input 1 dB compression point (IP1 dB) of -15 dBm and an input third-order intercept point (IIP3) of -1.62 dBm were measured (this latter value is stable between 2 and 6 GHz). The IIP3 value increases linearly with the optical losses up to 10 dB, with a slope equal to 2 showing the limitation of the O/E receiver; beyond 10 dB, the IIP3 remains stable and close to 20 dBm.

B. Digital Characterization of the RoF Link

In order to identify the best parameters of the RoF link, we study its performance in terms of EVM by varying the RF input power, the laser bias current, and the optical losses. The experimental results are reported in Figs. 6 and 7.

Without optical loss, the minimum EVM equals 13.4%. This value is observed for a 4 mA laser bias current and a -17.1 dBm

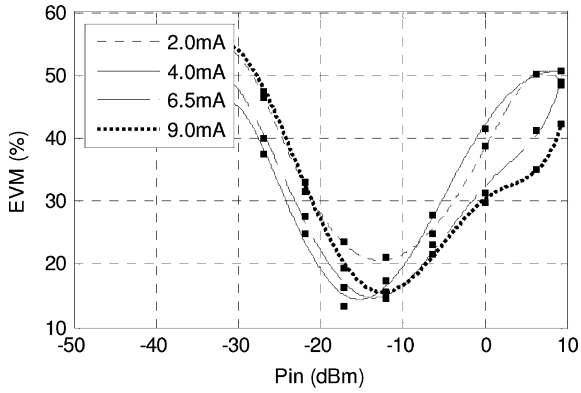

Fig. 6. Measured EVM versus RF input power for different laser bias currents. The optical loss is fixed to 0 dB.

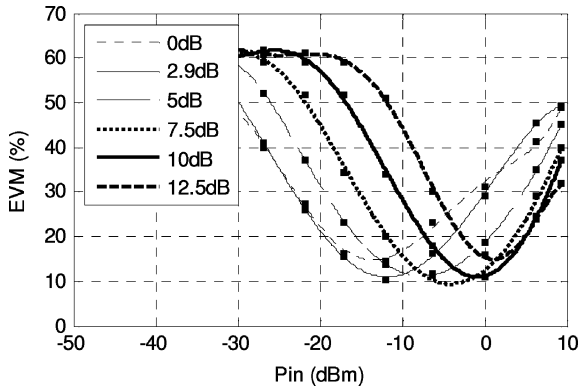

Fig. 7. Measured EVM versus RF input power for different optical losses. The laser bias current is fixed to 6.5 mA.

RF input power. This RF power corresponds to the IP1 dB parameter of the RoF link. For an RF power of -15 dBm, the results for the different laser bias currents are similar, except for 2 mA due to its closeness to the threshold current of the laser (1 mA), resulting in higher RIN, up to -120 dBc/Hz. Compared to the reference link, the minimum EVM has increased by 9.4%.

According to Fig. 7, the larger the optical losses, the higher the RF laser input power must be to attain the minimum EVM. For high RF input power, we observe the effects of the nonlinearity on the O/E receiving part; conversely, the nonlinearity of E/O emitting part does not affect the system because for all the optical losses the shape of the curves remains identical. These results are in agreement with the evolution of the IIP3 versus the RF input power. For lower RF power, the EVM rise is due to reduced SNRs, because the RIN and the reception noises are dominant. Finally, for a given value of optical losses, the EVM remains stable at its minimum over a range of 6 dB RF input power.

The curve in Fig. 8 shows the RF input power leading to the minimum EVM as a function of the optical losses. The measured results can be well fitted by a straight line of slope of 1.3 (dashed line), while a line of slope of 2 is expected as the electrical losses correspond to the double of the optical losses when they are expressed in logarithmic scale. The straight line fits quite well the central part of the experimental curve. However, at the beginning of the curve, the slope is lower because of

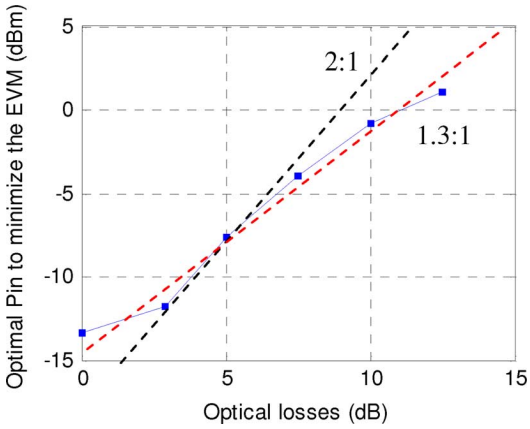

Fig. 8. Optimal RF input power leading to a minimal EVM value versus optical losses for a 6.5 mA laser bias current; continuous line corresponds to measurements and dashed lines to linear approximation and linear fitting of the measurements.

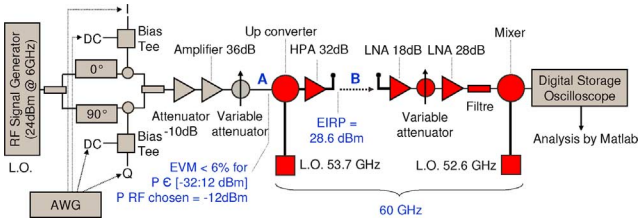

Fig. 9. 60 GHz radio-wireless link according to the IEEE 802.15.3c standard with free-space propagation.

predominant noises at low RF input level on one hand and the saturation of the TIA of the PIN photodiode at high RF input level on the other hand. In the final part of the curve, the laser nonlinearity impacts the slope.

IV. Characterization of Signal Transmission at an IFoF Tunnel

A. Implementation of a Single Millimeter-Wave Radio Link

The setup depicted in Fig. 9, used as the baseline, transmits IEEE 802.15.3c standard millimeter-waves in free space. The radio IF-OFDM signal is unchanged from Fig. 4; except that the center frequency is shifted from 5 to 6 GHz. The power of the IF-OFDM signal delivered is fixed at -12 dBm, the best experimental value achieved at the input of the first mixer (point A). This signal is up-converted to 59.7 GHz, in the frequency range corresponding to the second channel of the unlicensed millimeter-wave band (see Fig. 1).

At the radio emitter, an 8.6 dBm power is applied to a *V*-band horn antenna with 20 dB gain. The equivalent isotropically radiated power (EIRP) is 28.6 dBm, very close to the typical EIRP of commercial devices, i.e., 27 dBm (see Section V), and in agreement with the maximum EIRP allowed in Europe, i.e., 40 dBm mean [7], [8]. After a first hop in free space (point B), the signal is received by a second antenna and boosted by two low noise amplifiers (LNAs). The radio signal is then downconverted in order to be captured by the digital storage oscilloscope.

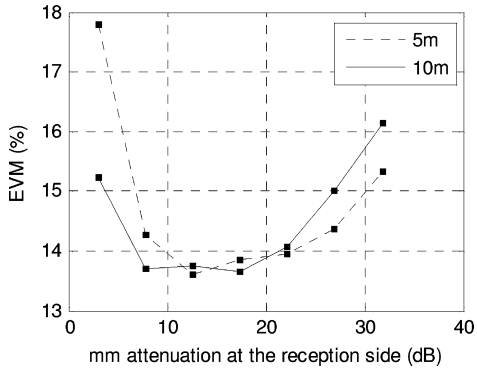

Fig. 10. EVM versus millimeter-wave attenuation at the receiver.

Fig. 10 represents the EVM at the radio receiver as a function of the millimeter-wave attenuation, introduced by a variable attenuator placed before the downconverted mixer, and for two fixed free-space distances, 5 and 10 m.

No significant variation can be observed between the two tested distances, just a reception attenuation shift equivalent to the loss difference between the two propagation distances. Indeed, the two considered distances correspond to free-space losses equal to 82 and 88 dB for 5 and 10 m, respectively (neglecting additional losses due to oxygen absorption). The EVM remains close to 14% over a 10 dB attenuation range. For shorter free-space distances, 1 m, for example, we have checked that the first LNA at the reception side does not saturate and that the millimeter-wave attenuator can adjust sufficiently the RF power.

Between 5 and 10 m free-space propagation distances, the optimal total millimeter-wave gain at the reception is 30 dB, plus 20 dB antenna gain, i.e., a total gain of 50 dB that does not compensate entirely the free-space propagation losses.

B. Implementation of an Electrical Repeater at 60 GHz.

The setup considered in Fig. 11 represents a repeater without RoF link. This setup allows us to check if the system tolerates the losses and distortions corresponding to two air links. The upper part in Fig. 11 is identical to the setup in Fig. 9.

After a first hop in free space, the signal is picked up by a horn antenna with 20 dB gain. A 28 dB LNA and a 32 dB high-power amplifier (HPA) boost the received signal. This radio signal is then downconverted to IF at 4.5 GHz and attenuated by 15 dB in order to simulate the RoF link behavior. Finally, the IF signal is upconverted to realize the second hop at 60 GHz. Finally, the received signal is analyzed on the oscilloscope.

The S21 parameter of the RoF link has been evaluated experimentally for a laser bias current of 6.5 mA. This latter is stable up to 6 GHz:

$$\mathrm{S21\ (dB)} = 2 \times \text{ optical losses} - 3\,\mathrm{dB}. \qquad (1)$$

To optimize the IF power applied to the upconverter, an attenuation of 15 dB is necessary for P3 corresponding approximately to a zero-optical loss RoF link. Indeed, as we have 0 dBm before P3 (see Fig. 11), an attenuation of 14 dB is needed to obtain the optimum IF power at the laser input (see Fig. 8). Moreover, 3 dB RF losses are added for the S21

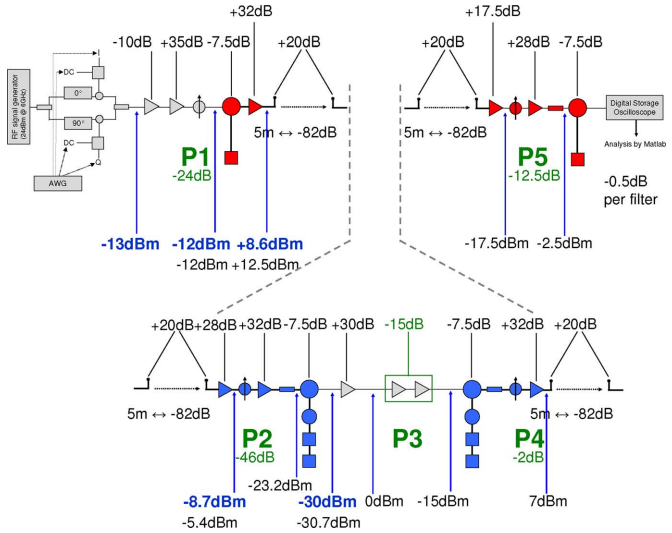

Fig. 11. Link budget for the radio tunnel at 60 GHz. P1 to P5, the different variable parameters, above the figure the RF gain, below in bold the measured power values, and below in regular the theoretical power values.

parameter (Formula 2). Finally, to simulate a RoF link without optical loss, 17 dB RF attenuation is required $(14\text{ dB} + 3\text{ dB})$.

Cascaded amplifiers and variable attenuators allow the optimization of the power applied not only to the input of each mixer (parameters P1, P2, P3, and P5), but also to the second 60 GHz air hop (parameter P4). The free-space distance, parameter P6, is fixed at 5 m for the two hops.

The EIRPs for these two air hops are, respectively, 28.6 and 27 dBm. For the configuration in Fig. 11, the measured EVM is 18.5%. The introduction of the electric repeater has increased the EVM by only 4.5%, thanks to the parameters optimization along the link.

C. Implementation of a RoF Tunnel at 60 GHz

The RF attenuator of the last configuration in Fig. 11 is replaced by the RoF link in Fig. 5 in this final step. A 300 m OM3 MMF and an optical attenuator are inserted; together they present 2.2 dB of intrinsic optical losses.

We fix the laser IF input power at -10 dBm, i.e., the optimal value to minimize the EVM for 4 dB optical losses according to Fig. 8. EVM are measured by varying the optical losses between 2 and 6 dB. This last value corresponds to the worst case for a point-to-point RoF link in an HAN. In this worst case, as the photodiode delivers an IF power of -22.7 dBm at the upconverter, the EIRP is then 19.3 dBm for the second hop and the received power is -62.7 dBm respecting the sensitivity of -65 dBm of the commercial HDMI transmitters from Gefen (cf., Section V).

Finally, we obtain the results of Table II. The measured EVM remains always below 25%. It corresponds to a theoretical bit error rate (BER) better than 10^{-5} [18], i.e., error-free transmission after coding implementation.

Fig. 13 represents the measured IF power spectrum at the receiver, for 3.2 dB total optical losses and 23.94% average EVM.

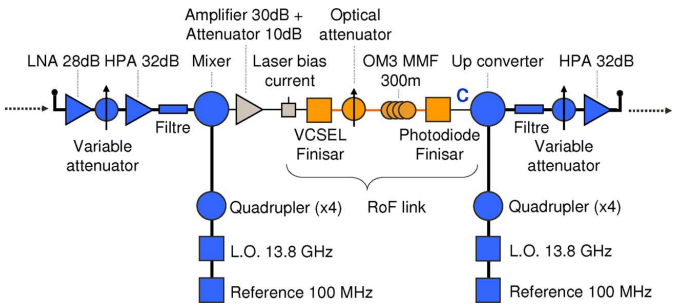

Fig. 12. RoF tunnel placed between the two hops in the air.

TABLE II
EVM (%) AS A FUNCTION OF THE TOTAL OPTICAL LOSSES FOR 300 mLENGTH OM3 MMF AND FOR $(5\text{ m} + 5\text{ m})$ AIR HOPS

Optical losses (dB)	EVM (%)
2.2	24.32
3.2	23.94
4.2	24.15
5.2	25.05

TABLE III
EVM AS A FUNCTION OF THE FREE-SPACE LENGTH

Distance (P6)	EVM (%)
5m + 5m	25.47
5m + 2m	22.52
2m + 5m	22.47

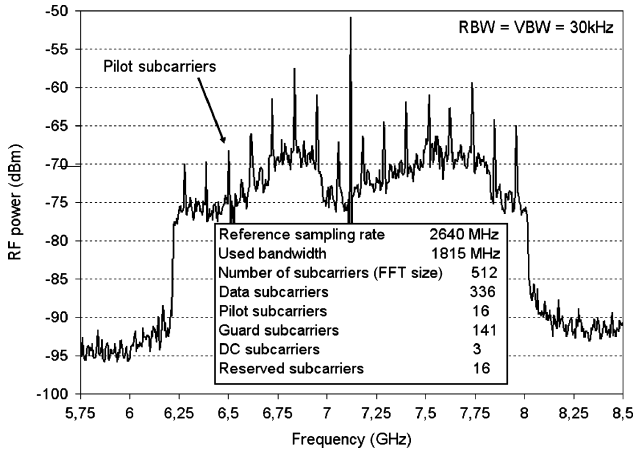

Fig. 13. Measured OFDM signal spectrum of IEEE 802.15.3c HSI mode at the receiver.

The two LOs of the optical tunnel working at the same frequency, 55.2 GHz; the center-received frequency is

$$6\text{ GHz} + 53.7\text{ GHz (1st LO)} - 52.6\text{ GHz (4th LO)} = 7.1\text{ GHz}. \quad (2)$$

Because of the large bandwidth of the standard channel, the received spectrum is slightly bumpy. A ripple of about 7 dB is introduced by the cumulated frequency responses of the RF circuits along the system. Nevertheless, the 16 pilot subcarriers

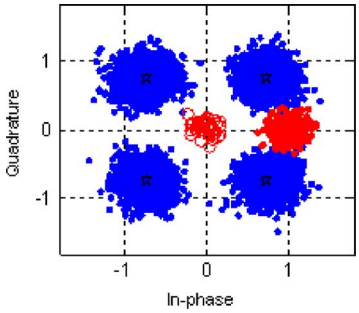

Fig. 14. QPSK constellation diagram in $(1,1)$, $(1,-1)$, $(-1,-1)$, and $(-1,1)$ with null subcarriers in $(0,0)$ and pilot subcarriers in $(1,0)$.

are clearly visible. The corresponding instantaneous EVM is 22.37% (see Fig. 14).

The signal has a bandwidth of 1.815 GHz with an average level of -72 dBm. As the bandwidth used on the spectrum analyzer is 30 kHz, the signal power is

$$\mathrm{P} = -72\,\mathrm{dBm} + 10\,\log_{10}(1.815\times10^{9}/30\times10^{3}) \sim -24\,\mathrm{dBm}. \quad (3)$$

This spectrum measurement was performed after the other measures, when the second amplifier and the variable attenuator of the reception stage have been removed. So, this value of -24 dBm is consistent with Fig. 11. The average noise level of the spectrum analyzer is -96 dBm, and the minimal carrier-to-noise ratio (CNR) is:

$$\mathrm{CNR\,min} = -75\,\mathrm{dBm} - (-90\,\mathrm{dBm}) = 15\,\mathrm{dB}. \quad (4)$$

A single RoF link with two different hop lengths has been also investigated. The configuration is the same as above, except that P parameters of Fig. 11 are optimized to simulate an amplifier with an automatic gain control after the first and the second hops in the air.

Measurements show identical results for 5 m+2 m and 2 m+5 m configurations. No free-space link configuration leads to larger damages on the system. In the worst wireless link case, the EVM is near the authorized BER limit.

V. IFoF Link Between Two Commercial WirelessHD Devices

Finally, a real-time transmission between two commercial Wireless-HD devices working at 3 Gb/s has been carried out. The main properties of these devices from Gefen are a transmitted power of 27 dBm and a receiver sensitivity of -65 dBm. An uncompressed 1080i video from Blu-ray player is displayed on an HD screen (cf., Fig. 15). The optical tunnel allows two wireless devices located in two rooms far away from each other to communicate as if they were in line of sight. The setup shown in Fig. 16 is similar to that in Fig. 12, except that two paths work in parallel: one for the downlink and other for the uplink.

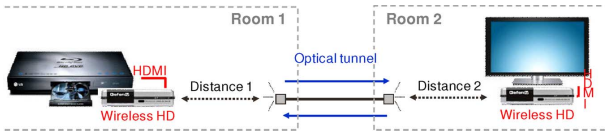

Fig. 15. Real-time bidirectional WirelessHD transmission through the RoF tunnel.

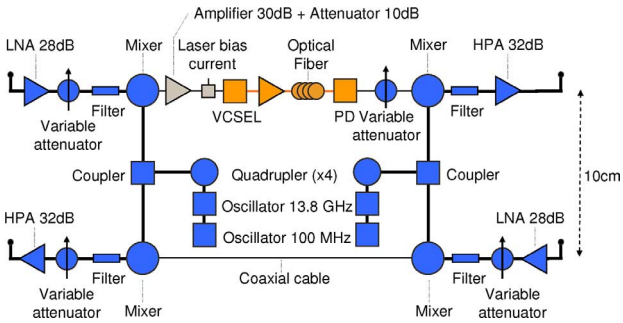

Fig. 16. Implemented bidirectional radio tunnel. Only the HRP WirelessHD signal (downlink) uses optical propagation.

TABLE IV
General Parameters of the HRP

Parameter	Value
Reference sampling rate	2.538 GSa/s
Used bandwidth	1.76GHz
Number of subcarriers (FFT size)	512
Data subcarriers	336
Pilots subcarriers	16
DC subcarriers	3
Null subcarriers	157

The downlink channel is a high data rate transmission called high-rate physical layer (HRP), whereas the uplink channel is at a low data rate for monitoring and it is called low-rate physical layer (LRP) [4]. LRP signal is also present over the downlink, but only temporarily. Both are OFDM signals, but with different physical characteristics. The HRP signal, based on the IEEE 802.15.3c A/V mode is also very close to the IEEE 802.15.3c HSI mode as it can be observed by comparing the general parameters of Table IV and Fig. 13. The HRP signal uses OFDM modulation with QPSK at 2.856 Gb/s PHY rate (1.904 Gb/s data rate) and uses the second channel of the millimeter-wave band as the radio signals of the previous parts. RoF is implemented only for the downlink, whereas the low data rate uplink uses a coaxial cable.

Even if radio systems operate in half-duplex, a RoF transparent tunnel transmits and receives simultaneously. A 10 cm distance between the adjacent Tx and Rx directional antennas is sufficient to avoid coupling issues. Otherwise, strong perturbations to the radio environment can happen.

The free-space lengths are fixed to 5 m plus 5 m. The bidirectional transmission was successful over both a 50 m length OM2 MMF and a 100 m length OM2 MMF, but the system has failed to operate with a 300 m length OM3 fiber probably due to restriction inside the radio medium access control layer [19].

Indeed, experimentally, we found a limit of 107 m length fiber. So, the propagation time cannot exceed $\sim$0.5 μs. Deeper investigations have shown that this delay corresponds to the total propagation time over the downlink and the uplink. Therefore, the system can operate with 50 m length fibers for both the downlink and the uplink.

The OM2 fiber length is fixed to 100 m. To verify the robustness of the link, an RF attenuator is added to the output of the photodiode. The RF attenuation can vary from 0 to 27 dB, beyond the connection stops.

A critical point for the WirelessHD transmission based on the IEEE 802.15.3c specification is the accuracy of LOs. According to the IEEE 802.15.3c standard, the transmitted center frequency tolerance shall be ± 25 μHz/Hz maximum, corresponding to ± 90.72 kHz at 60.48 GHz. We have measured the transmitted center frequency tolerance of the used commercial WirelessHD devices by changing the frequency of one LO of the optical tunnel, simulated by an RF signal generator. The transmission is interrupted when the 13.8 GHz oscillator is outside the window [13.8 GHz–38 kHz; 13.8 GHz+42 kHz]. This corresponds to an accuracy of ± 160 kHz with an LO at 55.2 GHz.

VI. Conclusion

The rise of the data rates in the HAN and the users demand for wireless solutions naturally lead to RoF technology. This paper has demonstrated that RoF systems can meet these needs. Indeed, real-time transmission between two commercial WirelessHD devices at 3 Gb/s has been achieved over 50 m, typical HAN size, and 100 m OM2 fiber lengths. To cover the whole house, more advanced RoF network architectures are under study, as the multipoint-to-multipoint infrastructure based on a passive optical splitter [20], [21]. For a massive adoption of the RoF technology, an advanced integration of the RoF transducers is also under consideration.

References

[1] B. Charbonnier, H. Wessing, and M. Popov, "Home networking requirements," presented at the presented at the IPHOBAC Workshop, Duisburg, Germany, May 2009, (invited paper).

[2] *Part 11: Wireless LAN Medium Access Control (MAC) and Physical Layer (PHY) Specifications. Amendment 5: Enhancements for Higher Throughput*, IEEE 802.11n, Oct. 2009.

[3] *Wireless Medium Access Control (MAC) and Physical Layer (PHY), Specifications for High Rate Wireless Personal Area Netwoks (WPANs)*, IEEE 802.15.3c, Oct. 2009, Version 1.0a.

[4] WirelessHD Specification Version 1.1 Overview May 2010 [Online]. Available: www.wirelesshd.org, WirelessHD

[5] IEEE 802.11ad, May 2010 [Online]. Available: www.ieee802.org/11

[6] WiGig [Online]. Available: http://wirelessgigabitalliance.org

[7] *Use of the 57–64 GHz Frequency Band for Point-to-Point Fixed Wireless Systems*, ECC Recommendation (09)01, 2009.

[8] *Use of the 64–66 GHz Frequency Band for Fixed Service*, ECC Revised Recommendation (05)02, 2009.

[9] J. Guillory, P. Guignard, F. Richard, L. Guillo, and A. Pizzinat, "Multi-service home network based on hybrid electrical & optical multiplexing on a low cost infrastructure," presented at the presented at the OSA OPC Access Netw. In-House Commun. Conf., Karlsruhe, Germany, Jun. 2010.

[10] A. Chowdury, H. C. Chien, Y. T. Hsueh, and G. K. Chang, "Advanced system technologies and field demonstration for in-building optical-wireless network with integrated broadband services," *J. Lightw. Technol.*, vol. 27, no. 12, pp. 1920–1927, Jun. 2009.

[11] A. Ng'oma, D. Fortusini, D. Parekh, W. Yang, M. Sauer, S. Benjamin, W. Hofman, M. C. Amann, and C. Chang-Hasnain, "Performance of a multi-Gb/s 60 GHz radio over fiber system empoying a directly modulated optically injection-locked VCSEL," *J. Lightw. Technol.*, vol. 28, no. 6, pp. 2436–2444, Aug. 2010.

[12] C. T. Lin, E. Z. Wong, W. J. Jiang, P. T. Shih, J. Chen, and S. Chi, "28 Gb/s 16-QAM OFDM radio-over-fiber system within 7 GHz license-free band at 60 GHz using all-optical up-conversion," presented at the presented at the Conf. Lasers and Electro-Opt., Baltimore, MD, May 2009, Paper CPDA8.

[13] A. Ng'oma, P. T. Shih, J. George, F. Annunziata, M. Sauer, C. T. Lin, W. J. Jiang, J. Chen, and S. Chi, "21 Gbps OFDM wireless signal transmission at 60 GHz using a simple IMDD radio-over-fiber system," presented at the presented at the IEEE OSA/Opt. Fiber Commun. Conf./ Collocated Natl. Fiber Opt. Eng. Conf., San Diego, CA, 2010, Paper OTuF4.

[14] C. T. Lin, J. Chen, P. T. Shih, W. J. Jiang, and S. Chi, "Ultra-high data-rate 60 GHz radio-over-fiber systems employing optical frequency multiplication and OFDM formats," *J. Lightw. Technol.*, vol. 28, no. 16, pp. 2296–2306, Aug. 2010.

[15] F. Lecoche, E. Tanguy, B. Charbonnier, H. W. Li, F. Van Dijk, A. Enard, F. Blache, M. Groix, and F. Mallécot, "Transmission quality measurement of two types of 60 GHz millimeter-wave generation and distribution system," *J. Lightw. Technol.*, vol. 27, no. 23, pp. 5469–5474, Dec. 2009.

[16] A. Pizzinat, I. Louriki, B. Charbonnier, F. Payoux, S. Meyer, M. Terré, C. Algani, A. L. Billabert, J. L. Polleux, C. Sillans, H. Jaquinot, S. Bories, Y. L. Guennec, and G. Frog, "Low cost transparent radio-over-fibre system for UWB based home network," presented at the presented at the Eur. Conf. Opt. Commun., Bruxelles, Belgium, 2008, Paper Tu.3.F.1.

[17] J. Guillory, S. Meyer, I. Siaud, A. M. Ulmer-Moll, B. Charbonnier, A. Pizzinat, and C. Algani, "Radio over fiber architectures, future Multi-Gigabit wireless systems in the home area network," *IEEE Veh. Technol. Mag.*, vol. 5, no. 3, pp. 1556–6072, Sep. 2010.

[18] R. A. Shafik, M. S. Rahman, and A. R. Islam, "On the extended relationships among EVM, BER and SNR as performance metrics," in *Proc. 4th Int. Conf. Electr. Comput. Eng.*, Dec. 2006, pp. 408–411.

[19] B. L. Dang and I. Niemegeers, "Analysis of IEEE 802.11 in radio over fiber home networks," in *Proc. IEEE Conf. Local Comput. Netw. 30th Anniversary*, 2005, pp. 744–747.

[20] J. Guillory, S. Meyer, B. Charbonnier, T. Derham, and S. Roblot, "Radio over fiber for an optimal 60 GHz home area network," in *IEEE 11-10-0011-01-00ad Conf. Call*, Jan. 2010 [Online]. Available: https://mentor.ieee.org/802.11/dcn/10/11-10-0011-01-00ad-radio-over-fiber-for-an-optimal-60-ghz-home-area-network.ppt

[21] J. Guillory, S. Meyer, I. Siaud, A. M. Ulmer-Moll, B. Charbonnier, A. Pizzinat, and C. Algani, "RoF architectures for multi-gigabit wireless systems in the home area network," in *Proc. 24 WWRF WG5*, Apr. 2010, pp. 1–9.